Crystallization of Poly(hydroxybutyrate-*co*-hydroxyvalerate) in Wood Fiber-Reinforced Composites

VERONIKA E. REINSCH, STEPHEN S. KELLEY

National Renewable Energy Laboratory, 1617 Cole Blvd., Golden, Colorado 80401

Received 14 August 1996; accepted 20 November 1996

ABSTRACT: Wood fiber-reinforced composites were prepared from poly(hydroxybutyrate) (PHB) and poly(hydroxybutyrate-*co*-hydroxyvalerate) (PHB/HV) copolymers containing 9 and 24% valerate. The effects of fibers on crystallization were investigated. Thermomechanical pulp, bleached Kraft fibers, and microcrystalline cellulose filler were used as the reinforcing phase. The crystallization of PHB/HV in composite materials was examined using Modulated Differential Scanning Calorimetry (MDSC) and hot-stage microscopy. Hot-stage microscopy showed that polymer crystallites are nucleated on the fiber surface and that the density of nuclei was greater in fiber-reinforced composites than in unfilled material. Dynamic crystallization experiments showed that bleached Kraft, thermomechanical pulp, and microcrystalline cellulose increased the crystallization rate of PHB and PHB/HV both from the glass and melt. However, ultimate crystallinity determined from the heat of crystallization was the same in unreinforced and reinforced materials. The kinetics of PHB/HV crystallization were examined using nonisothermal Avrami-type analysis. Unreinforced and Kraft-reinforced PHB were characterized and compared with unreinforced PHB/9%HV. The Avrami exponent of crystallization, related to nucleation mechanism and growth morphology, is 2.0 for unreinforced PHB, 2.8 for kraft-reinforced PHB, and 3.0 for unreinforced PHB/9%HV. © 1997 John Wiley & Sons, Inc. J Appl Polym Sci **64:** 1785–1796, 1997

INTRODUCTION

Because plastics compose an estimated 18% by volume of municipal solid waste,[1] the development of commercially viable biodegradable plastics is an important effort toward the preservation and revitalization of our global environment. A class of biodegradable plastics receiving considerable attention is poly(hydroxyalkanoates) or PHAs, in particular poly(3-hydroxybutyrate) (PHB) and copolymers poly(3-hydroxybutyrate-*co*-3-hydroxyvalerate) (PHB/HV).[2–11] Although PHAs are biodegradable—microorganisms are able to rapidly degrade PHB and PHB/HV to carbon dioxide and water[6]—their rate of chemical hydrolysis is slow. This is an advantageous combination of properties. These plastics are produced by microbes (including soil bacteria, estuarine microflora, blue green algae, and various photobiological systems) as a natural part of their metabolism.[10] Although the proportion of PHA in cells typically is below 30%, under fermentation conditions of carbon excess and nitrogen limitation, PHA can compose as much as 70% of dry cell weight.[11] The typical feedstock for PHB production is glucose. When propionic acid is added to the growth medium during conditions of nitrogen limitation, the polymer produced is PHB/HV copolymer. Bacterially produced PHB/HV copolymers have been demonstrated to be randomly sequenced.[12]

The chemical structures of the HB and HV repeat units are shown below.

Correspondence to: S. S. Kelley.

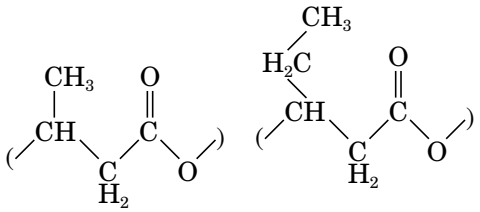

HB HV

PHB and PHB/HV are crystallizable thermoplastic polyesters. Despite the difference in the size of repeat units, PHB/HV copolymers exhibit the interesting property of cocrystallization. That is, both HV units and HB units are included in the crystalline unit cell. However, only one characteristic unit cell is observed for most copolymer compositions. Copolymers containing less than 40% HV units crystallize in the PHB unit cell, while copolymers containing 50% or more HV units crystallize in the PHV unit cell.[12,13] Copolymers with HV content between 40 and 50% exhibit crystals with both unit cells.

PHB has attracted some commercial interest because it possesses properties similar to synthetic thermoplastics such as polypropylene.[1] However, PHB is little used commercially because of its brittle behavior[7] and lack of melt stability.[6] These drawbacks have furthered interest in PHB/HV copolymers, which are tougher and have greater melt stability.[10] However, crystallization rates of copolymers are very slow compared with the time scale of most industrial molding and fabrication processes. Slow crystallization rates are related to slow nucleation rates and to slow linear growth rates resulting from inclusion of, for example, HV units in the PHB crystalline lattice.

The development of commercial applications for PHAs requires improving crystallization and processing behavior, reducing overall costs, and further enhancing mechanical properties. One approach for overcoming these limitations is to incorporate fiber reinforcements into the polymer to create reinforced composites. In addition to an expected improvement of mechanical properties, some studies have shown that incorporating reinforcing fibers in other crystallizable thermoplastic polymers can significantly increase the crystallization rate of semicrystalline thermoplastic polymers.[14,15] However, no previous study has described the effect of reinforcing fibers on the crystallization of PHAs. This study quantified the effects of fiber reinforcement on the crystallization rate of PHAs.

EXPERIMENTAL

Methods and Materials

The PHA samples obtained for this study were PHB homopolymer, PHB/9%HV (random copolymer with 9% valerate repeat units), and PHB/24%HV (random copolymer with 24% valerate repeat units). Proton nuclear magnetic resonance (^{1}H-NMR) spectroscopy was run on a Varian 300 MHz spectrometer using deuterated chloroform as a solvent to determine PHA copolymer composition. Thirty-two scans were acquired using a 5-s delay time and tetramethylsilane (TMS) as a reference.

Wood fiber-reinforced composites were produced by melt compounding in a Brabender Plasticorder. Unbleached thermomechanical pulp (TMP) derived from southern pine, bleached Kraft fibers (also from southern pine), and microcrystalline cellulose (MCC) were evaluated as the reinforcing component. Bleached Kraft filler was ground in a Wiley mill prior to compounding so that fibers would disperse adequately in the polymer matrix. Unreinforced PHB, PHB/9%HV, and PHB/24%HV were also compounded so that any observed differences in crystallization may be conclusively attributed to the nature of the reinforcing phase, and not to melt compounding effects. Table I shows the fiber loading of the various composites prepared. Composites of PHB were melt compounded at 200°C, and composites of PHB/9%HV and PHB/24%HV at 195°C. The total time of melt processing was 10 min for all samples and the rotor speed was 30 rpm.

Following compounding, composite sheets were prepared by melt pressing chips of compounded material on a hot press at 190°C and 200 psi for 3 min. Specimens weighing approximately 10 mg were cut from these sheets for examination using Modulated Differential Scanning Calorimetry (MDSC). Specimens were sealed in an aluminum sample pan, melted at 190°C for 3 min, and then quenched on dry ice to produce a completely amorphous sample. The quenched specimen was then heated in the MDSC at a rate of 5°C/min to 200°C (190°C for 9 and 24% HV copolymers), and then cooled at 5°C/min to 0°C, and then heated at 5°C/min to 220°C. The temperature modulation had an amplitude of $\pm$0.79°C and a period of 60 s.

A second set of specimens was quenched to room temperature and allowed to crystallize slowly. The same MDSC protocol as described

Table I Composite Systems Prepared, Including Matrix Type, Fiber Type and Treatment, and Fiber Loading

Polymer Matrix	Neat	Fiber Reinforcement (wt %)		
		TMP[a]	Bleached Kraft	MCC[b]
PHB[c]	0	10, 20, 40	10, 20, 40	20
PHB/9% HV[d]	0	10, 20, 40	10, 20, 40	20
PHB/24% HV[d]	0	20	10, 20, 40	20

[a] Thermomechanical pulp.
[b] Microcrystalline cellulose.
[c] Poly(hydroxy butyrate).
[d] Poly(hydroxy butyrate-*co*-hydroxy valerate).

above was applied to these crystalline samples to quantify the melting behavior of slowly crystallized specimens.

A series of dynamic melt crystallization experiments were performed at various heating rates in order to quantify the kinetics of dynamic melt crystallization. Standard differential scanning calorimetry (DSC), rather than MDSC, was employed. Sample preparation for DSC (prior to introduction of the sample in the calorimeter) was identical to that for MDSC, described above. Unreinforced PHB, unreinforced PHB/9%HV, and kraft fiber-reinforced PHB specimens were examined. Samples were heated at 20°C/min to 200°C (190°C for PHB/9%HV), then cooled at the desired cooling rate to 0°C. Cooling rates varied from 20°C/min to 1°C/min. Three replicates were performed at each cooling rate.

Gel permeation chromatography (GPC) was used to measure the molecular weight of the PHB/24%HV samples. Both the as-received powder and melt-compounded composites were considered. Melt-compounded specimens were taken from the same samples as those used in the calorimetry experiments (both unreinforced and fiber reinforced). Tetrahydrofuran (THF) was used as the solvent. Monodisperse polystyrenes were used to calibrate two 8 × 300 mm, Hewlett Packard columns containing polystyrene–divinylbenzene copolymer gel (particle size 10 μm) with nominal pore diameters of 10^5 and 10^4 Å, respectively. The samples were run as 0.1% solutions, heated to ensure complete dilution, and filtered to remove fibers. Molecular weights of the PHB and PHB/9%HV samples were not measured owing to problems with the limited solubility in THF.

The crystalline morphology and nucleation behavior of fiber-reinforced PHB/HVs were investigated using optical microscopy. A light microscope equipped with a programmable hot stage was used to observe the formation of crystalline order, both from the glass and from the melt. Approximately 10 mg of polymer and 1 mg of fiber were placed between glass coverslips and melted on a hot plate at 200°C for 5 min under pressure. For studies of melt crystallization, the sample was then immediately moved to the hot stage where the temperature was maintained at the selected crystallization temperature. For studies of cold crystallization (crystallization from the glassy state), the sample was removed to dry ice until equilibrated, and then placed on the hot stage at the crystallization temperature of interest.

RESULTS AND DISCUSSION

Nuclear Magnetic Resonance Spectroscopy

The chemical composition of the PHA copolymers was determined by ^{1}H-NMR. The ^{1}H-NMR peak assignments for the PHB homopolymer and the PHA copolymers have been determined.[16,17] Methyl protons for the butyrate repeat unit are seen as a doublet at about 1.28 ppm, while the methyl protons for the valerate unit are seen as a triplet at about 0.88 ppm. The ratio of peak intensities was used to determine the molar composition of the copolymer. This analysis shows that PHB homopolymer contains no detectable traces of valerate units. The two copolymer samples contain 9 and 24% valerate, respectively. These compositions are similar to the copolymer compositions reported by the suppliers (8 and 24%, respectively).

Table II Effects of Melt Compounding at 195 to 200°C on the Molecular Weights and Polydispersity of Unreinforced and Fiber Reinforced PHB/24% HV

Reinforcing Phase and Loading	(wt %)	$\overline{M}_n$[a]	$\overline{M}_w$[b]	$\overline{M}_w/\overline{M}_n$[c]
Not heat compounded				
Neat	(0)	79,000	170,000	2.2
Heat compounded				
Neat	(0)	63,000	128,000	2.0
TMP[d]	(20)	66,000	133,000	2.0
MCC[e]	(20)	67,000	136,000	2.0
Bleached Kraft	(10)	64,000	129,000	2.0
	(20)	56,000	110,000	2.0
	(40)	58,000	110,000	1.9

[a] Number-average molecular weight.
[b] Weight-average molecular weight.
[c] Polydispersity.
[d] Thermomechanical pulp.
[e] Microcrystalline cellulose.

Gel Permeation Chromatography

The effects of melt compounding on the molecular weight of the PHB/24%HV samples are shown in Table II. Compounding at 195 to 200°C reduces the molecular weight of the PHB/24%HV samples by about 20–30%. The type or the amount of added filler did not affect the molecular weight of the samples. These observations confirm previous reports that PHB and PHB/HV are subject to rapid thermal degradation at temperatures above 200°C.[5,6]

Optical Microscopy

Optical microscopy observations of crystallization in unreinforced PHB and PHB/HVs indicate that crystal nuclei form sporadically through time. This type of nucleation is termed thermal nucleation. Thermal nucleation is often, although not always, associated with the formation of homogeneous nuclei. Homogeneous nucleation results from fluctuations in chain order, which produce nuclei of a critical size, rather than the formation of nuclei at foreign surfaces or impurities (known as heterogeneous nucleation). As bacterial polyesters are typically quite pure, the observation of thermal nucleation and conclusions regarding homogeneous nucleation mechanisms are not surprising.

The formation of crystalline order in fiber-reinforced systems is significantly different from that in the unreinforced systems. Figure 1(a) is an optical micrograph that shows the crystalline morphology of PHB/9%HV in the presence of a single bleached Kraft fiber after 2 min of crystallization from the melt. Polymer crystals have formed at the fiber surface and were growing outwards. At least 10 surface-nucleated crystals are apparent, while no bulk-nucleated crystals are observed. Figure 1(b) shows the same crystallization process after 2.5 min. A small crystallite formed in the bulk, and the surface-nucleated crystals grew significantly. Figure 1(c) shows crystallization after 5 min; the field appears completely crystalline and the crystalline morphology is dominated by surface-nucleated crystals.

Optical microscopy observations indicate that all kinds of fiber reinforcement have a significant nucleating effect on PHB and PHB/HV crystallization. Because of the high purity of these bacterial polymers, nucleation in the absence of foreign surfaces is typically very slow. In composites, adding fiber surfaces that nucleate the growth of polymer crystals has a significant effect on crystal morphology.

Modulated Differential Scanning Calorimetry

In MDSC, the traditional linear heating rate is replaced with a sinusoidal heating profile. Figure 2 shows a typical plot of temperature as a function of time for an MDSC scan performed at a heating

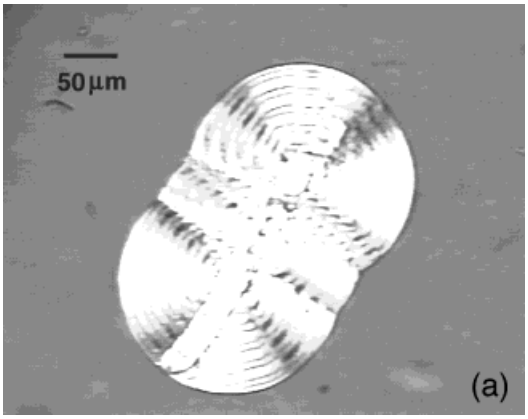

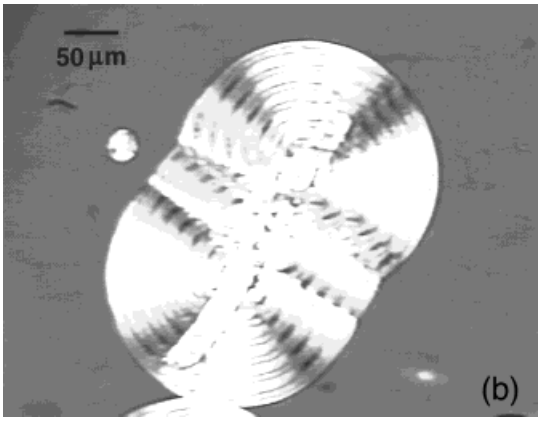

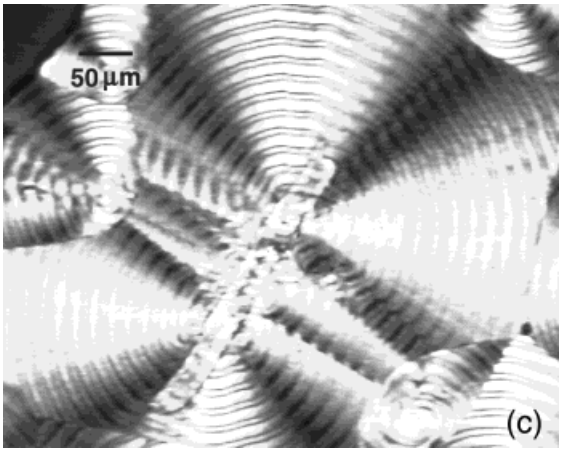

Figure 1 (a) Optical micrograph of isothermal crystallization at 70°C of PHB/9%HV in the presence of a single bleached Kraft fiber. Elapsed time is 2 min. (b) Optical micrograph of isothermal crystallization at 70°C of PHB/9%HV in the presence of a single bleached Kraft fiber. Elapsed time is 2.5 min. (c) Optical micrograph of isothermal crystallization at 70°C of PHB/9%HV in the presence of a single bleached Kraft fiber. Elapsed time is 5 min.

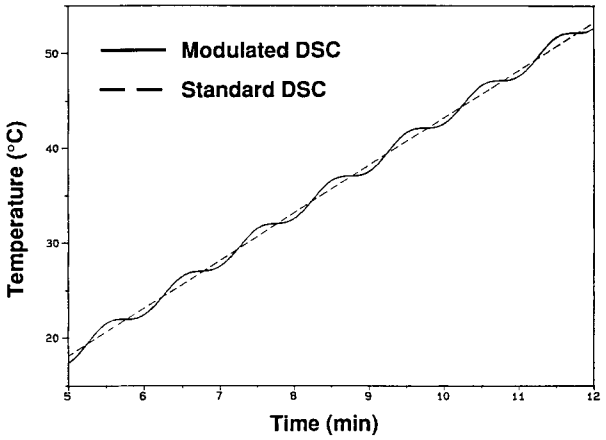

Figure 2 MDSC scan showing modulated temperature as a function of time.

rate of 5°C/min and a traditional DSC scan at 5°C/min. The temperature modulation in MDSC allows separation of the heat flow signal into thermodynamically reversing and nonreversing events. MDSC permits the separation of glass transition and melting events (reversing) from crystallization events (nonreversing).[18] The technique is particularly useful in the thermal analysis of polymers such as PHB and PHB/HVs, where both melting and crystallization events are believed to occur in the same temperature range.

Figure 3 shows a typical DSC scan of quenched PHB/9%HV. The scan shows glass transition, recrystallization (cold crystallization), and melting. Figure 4 shows an MDSC scan of the same material, with the separation of the heat flow signal

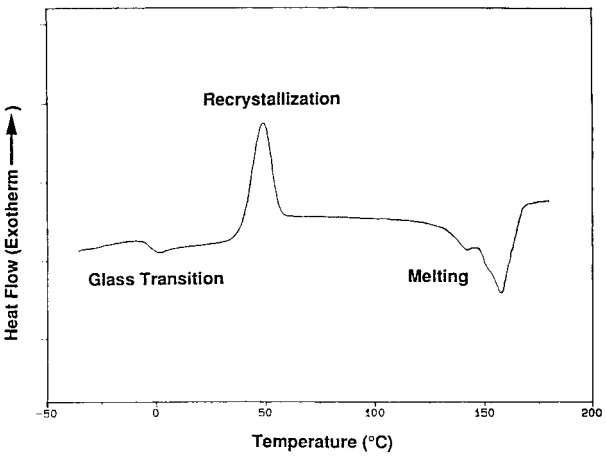

Figure 3 DSC scan of PHB/9%HV showing glass transition, recrystallization, and melting.

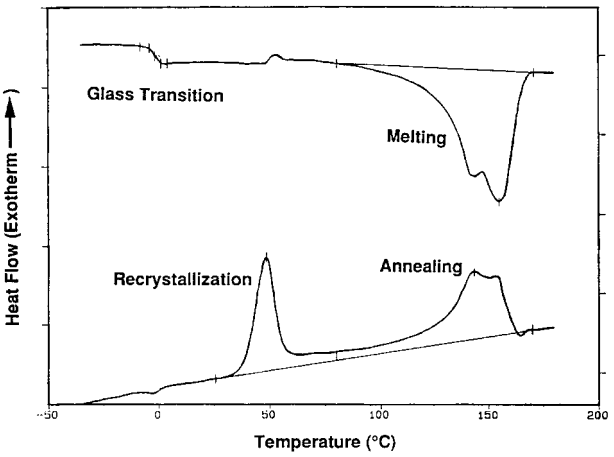

Figure 4 MDSC scan of PHB/9%HV with separation of the signal into thermodynamically reversing and nonreversing components. The reversing signal shows glass transition and melting, and the nonreversing signal shows recrystallization and annealing.

into reversing and nonreversing heat flow signals. This scan shows significant annealing in the same temperature region as melting. We can quantify the contributions of recrystallization and annealing to overall crystallization. The total heat flow due to exothermic events—crystallization and annealing—is only 7 J/g less than the heat flow due to melting, indicating that the sample had very little initial order and that the quenching process was very effective. It is also worth noting that problems with apparent baseline drift and complex melting behavior evident in the DSC scan disappear upon the separation of the melting and crystallization signals by MDSC. These improvements make MDSC very useful for the thermal analysis of PHAs.

Crystallization of Neat PHAs

As seen in Figure 4, an initial heating scan of quenched material displays a crystallization exotherm upon heating through the glass transition region. The temperature at the maximum height of this peak is taken to be the recrystallization, or cold crystallization temperature. After heating through the melting transition, the sample is cooled and crystallization from the melt is observed. The melt crystallization temperature is the temperature at the maximum height of the melt crystallization peak. It is important to note that the lower the recrystallization temperature, the greater the cold crystallization rate (for scans performed at the same cooling rate). Conversely, the higher the melt crystallization temperature, the greater the melt crystallization rate.

Figure 5 shows melt and cold crystallization temperatures as a function of copolymer composition (% of HV units). Melt crystallization temperature decreases with increasing HV content, reflecting a decrease in the rate of melt crystallization. Recrystallization temperature increases with increasing HV content, reflecting a decrease in the rate of crystallization from the glass. Thus, the rate of crystallization both from the melt and from the glassy state decreases with increasing HV content in the polymer. For all compositions of PHB/HVs considered, crystallization occurs in the unit cell characteristic of PHB.[13] The depression in crystallization rate with increasing HV content reflects the difficulty of incorporating HV units in crystals having a PHB unit cell. The incorporation of bulky HV units in the PHB crystal lattice slows both nucleation and linear growth rates of crystals.[2]

Melt Crystallization of Fiber-Reinforced PHAs

The melt crystallization temperature of various composites of PHB is given in Figure 6. The melt crystallization temperature of neat PHB is 90°C. The crystallization temperature of the fiber-reinforced composites is higher, reflecting an increased crystallization rate. This enhancement of crystallization rate is likely due to enhanced crystal nucleation at the fiber surface. Optical micrographs discussed above show the rapid development of crystal nuclei on the fiber surface. The

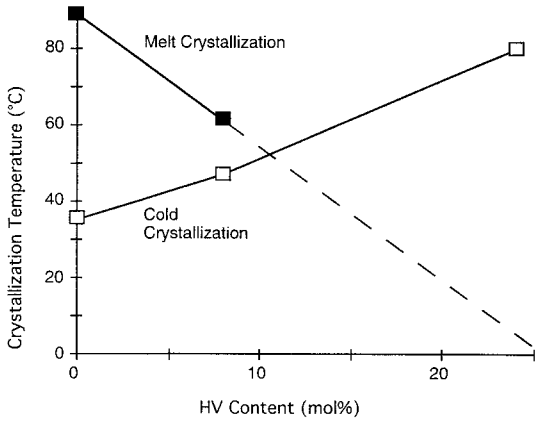

Figure 5 Melt crystallization temperature and cold crystallization temperature as a function of HV content in PHB/HV copolymers.

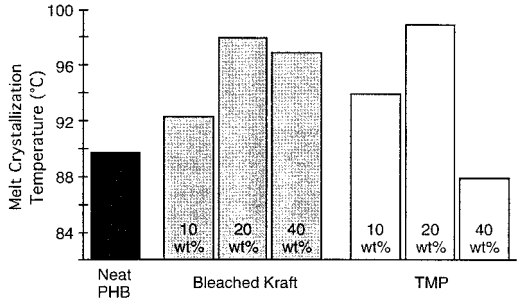

Figure 6 Melt crystallization temperature of PHB and fiber-reinforced PHB.

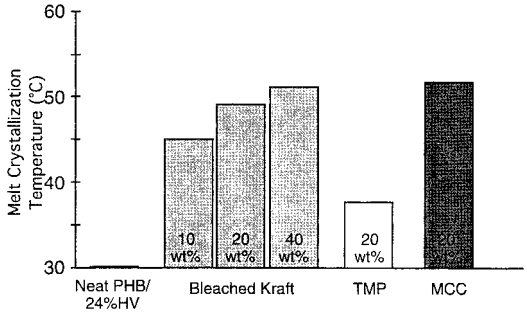

Figure 8 Melt crystallization temperature of PHB/ 24%HV and fiber-reinforced PHB/24%HV.

higher nucleation density at the fiber surface results in an increased effective nucleation rate, and this would be expected to increase the crystallization rate from the melt. Enhancement of crystallization rate appears to be more pronounced at greater filler contents, as would be expected if fiber surfaces nucleate crystallization. However, we also noted that crystallization rate decreased in the composite with the highest TMP content. This is the only composite system in which a decrease in crystallization rate was observed, and the depression in rate may reflect an aberration in processing this composite.

The melt crystallization temperature of composites of PHB/9%HV is shown in Figure 7. As in the case of PHB, fiber reinforcement significantly increased the crystallization temperature, reflecting an increased crystallization rate of PHB/ 9%HV. The melt crystallization temperature of fiber-reinforced PHB/9%HV is significantly greater than that of neat PHB/9%HV. As discussed above, the increased crystallization rate in fiber-reinforced systems is likely the result of greater crystal nucleation on the fiber surface. In PHB/9%HV composites, fiber loading does not significantly affect crystallization temperature.

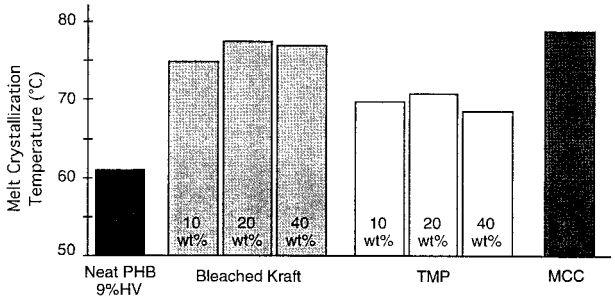

Figure 7 Melt crystallization temperature of PHB/ 9%HV and fiber-reinforced PHB/9%HV.

For loadings between 10 wt % and 40 wt %, the crystallization temperature is approximately the same. However, fiber type did have an effect. Bleached Kraft fibers and microcrystalline cellulose increased crystallization rate more than did TMP fibers. This trend is interesting, as the surfaces of bleached Kraft and MCC contain regions of crystalline cellulose, while the surface of TMP is likely to be covered by lignin and hemicelluloses. It is possible that fiber surface morphology plays a role in crystal nucleation on the fiber surface. Past studies of surface-nucleated crystallization indicate that fiber surface topography is a determining factor in the extent of nucleation, and studies of nucleating additives for PHAs indicate that crystal morphology of additives is a significant factor in nucleating efficacy.[11]

The melt crystallization of PHB/24%HV is shown in Figure 8 for various fiber-reinforced systems. The melt crystallization of neat PHB/ 24%HV is very slow and was not observed during cooling at 5°C/min from the melt to the glass transition temperature (T_g), but rather upon subsequent heating from T_g to the melt. For this reason, the melt crystallization temperature of the neat system appears off scale in Figure 8. Clearly, the melt crystallization temperature was significantly greater in the fiber-reinforced systems than in neat PHB/24%HV, reflecting a significantly increased crystallization rate. As in the case of PHB/9%HV composites, the bleached Kraft and MCC composites crystallized more rapidly than did composites with TMP filler. Again, this may be related to the more ordered surface of bleached Kraft and MCC as compared with TMP.

Cold Crystallization of Fiber-Reinforced PHAs

Figures 9, 10, and 11 show the recrystallization temperature of fiber-reinforced PHB, PHB/

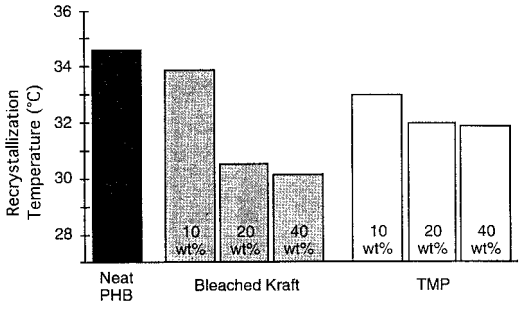

Figure 9 Recrystallization temperature of PHB and fiber-reinforced PHB.

9%HV, and PHB/24%HV, respectively. For all three matrices, fiber reinforcement depressed the cold crystallization temperature. This depression reflects an increased rate of cold crystallization. Optical microscopy observations (discussed earlier) of the crystallization of PHB and PHB/HVs in the presence of fibers reveal densely nucleated crystals on the fiber surface. The nucleation of crystals in the bulk, far from the fiber surface, is appreciable; however, the density on the fiber surface is much greater. This enhancement of nucleation rate is likely responsible for the observed increase in overall cold crystallization rate.

It is interesting that the effect of fiber reinforcement on recrystallization temperature is stronger in the copolymers PHB/9%HV and PHB/24%HV than in PHB. As discussed earlier, nucleation and crystal growth are significantly slower in PHB/HV copolymers, owing to the incorporation of HV units in crystals characteristic of PHB. Fiber surfaces act to reduce the critical nucleus size required for a stable nucleus, and this reduction in necessary nucleus size has a much more significant effect in the copolymers than in PHB.

As with melt crystallization, fiber loading affects crystallization rate. The increase in crystallization rate is greater at higher fiber loadings, as indicated by the lower melt crystallization temperature. This is the expected outcome of having more fiber surface area available for crystal nucleation. There are no significant trends with fiber type. In contrast to the observations in the melt crystallization studies, in cold crystallization bleached Kraft and MCC fillers do not have a greater effect on crystallization temperature than TMP.

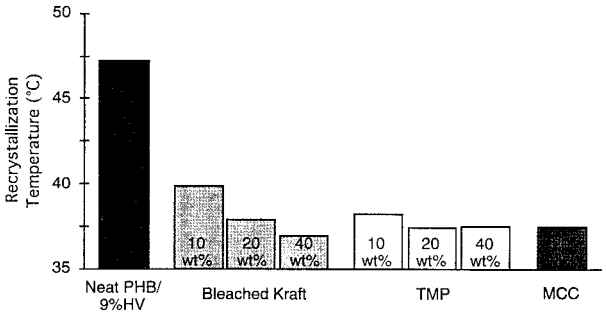

Figure 10 Recrystallization temperature of PHB/9%HV and fiber-reinforced PHB/9%HV.

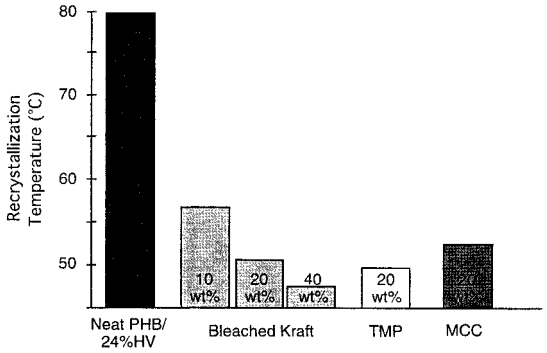

Figure 11 Recrystallization temperature of PHB/24%HV and fiber-reinforced PHB/24%HV.

Degree of Crystallinity

The degree of crystallinity achieved during crystallization, X, is defined as the heat of crystallization, ΔH_c, divided by the heat of crystallization of a theoretical perfect crystal of the same material, ΔH_f°. We will use a value of 130 J/g for the heat of crystallization of a perfect PHB crystal[2] and 123 J/g for the heat of crystallization of a perfect PHB/9%HV crystal (value interpolated from results presented in ref. 2). The heat of crystallization of 100% crystalline PHB/9%HV is less than that of 100% crystalline PHB, because of the inclusion of HV units by cocrystallization.

The degree of crystallinity for PHB and fiber-reinforced PHB is given in Table III. The heat of crystallization, ΔH_c, was determined by MDSC from the heat of fusion following crystallization, ΔH_f, minus the heat of annealing, ΔH_a. Table III shows that the degree of crystallinity is essentially the same in all systems. Although fiber reinforcement has a significant effect on crystallization temperature and crystallization rate, there is no effect on the ultimate crystallinity achieved. The small variation in ΔH values seen in Table

Table III Degree of Crystallinity and Heats of Fusion, Annealing, and Crystallization of Neat and 20% Fiber Reinforced PHB

PHB Material Tested	X[a]	Heat Flow (J/g) ΔH_f[b]	ΔH_a[c]	ΔH_c[d]
Neat	0.73	167	72	95
Fiber Reinforced (20 wt %)				
TMP[e]	0.75	158	61	97
MCC[f]	0.78	170	68	102
Bleached Kraft	0.79	167	64	103

[a] Degree of crystallinity, $\Delta H_c/\Delta H_f^0$.
[b] Heat of fusion.
[c] Heat of annealing.
[d] Heat of crystallization, $\Delta H_f - \Delta H_a$.
[e] Thermomechanical pulp.
[f] Microcrystalline cellulose.

III comes not only from the calorimeter signal but, more important, from uncertainty in the fiber content of the specimen examined by calorimetry. Local variation in fiber loading in melt compounded composites results in inaccuracy in the calculated quantity of polymer present in the small MDSC specimens.

Table IV shows the degree of crystallinity and heats of fusion, annealing, and crystallization for composites of PHB/9%HV. As in the case of PHB composites, the degree of crystallinity was approximately equal in all systems and was not significantly changed by the addition of reinforcing fibers. Although fiber reinforcement significantly increases the rate of PHB/9%HV crystallization, the final crystallinity was not significantly affected. It is important to note that although the heat of crystallization of PHB/9%HV composites is less than the heat of crystallization of PHB composites, the degree of crystallinity in the PHB and PHB/9%HV systems is approximately the same. Observed differences in degree of crystallinity are within the uncertainty in the heat flow measurements (typically 5 to 10 J/g, resulting primarily from inaccuracies in the amount of polymer present in the MDSC specimen, as mentioned above). Composites of PHB/24%HV (data not shown) also showed no effect of fiber reinforcement on degree of crystallinity.

Table IV Degree of Crystallinity and Heats of Fusion, Annealing, and Crystallization of Neat and 20% Fiber Reinforced PHB/9% HV

PHB/9% HV Material Tested	X	Heat Flow (J/g) ΔH_f[b]	ΔH_a[c]	ΔH_c[d]
Neat	0.69	136	51	85
Fiber Reinforced (20 wt %)				
TMP[e]	0.77	143	48	95
MCC[f]	0.76	140	46	94
Bleached Kraft	0.80	140	42	98

[a] Degree of crystallinity, $\Delta H_c/\Delta H_f^0$.
[b] Heat of fusion.
[c] Heat of annealing.
[d] Heat of crystallization, $\Delta H_f - \Delta H_a$.
[e] Thermomechanical pulp.
[f] Microcrystalline cellulose.

Table V Degree of Crystallinity[a] for Slow Crystallization at Room Temperature of PHB and PHB/9% HV Composites from the Amorphous State

Matrix	Neat	Fiber Reinforcement (20 wt %) TMP[b]	MCC[c]	Bleached Kraft
PHB[d]	0.71	0.71	0.70	0.73
PHB/9% HV[e]	0.62	0.73	0.72	0.72

[a] Degree of crystallinity, $\Delta H_c/\Delta H_f^0$.
[b] Thermomechanical pulp.
[c] Microcrystalline cellulose.
[d] Poly(hydroxy butyrate).
[e] Poly(hydroxy butyrate-*co*-hydroxy valerate).

Degree of crystallinity is given in Table V for neat and fiber-reinforced PHB and PHB/9%HV specimens that were crystallized slowly at room temperature (approximately 20°C above the glass transition temperature) for several months. The degree of crystallinity for all systems is close to 70%, and the variation among the results is within the uncertainty in the heat flow measurements. To evaluate the effect of crystallization rate on degree of crystallinity, the values for degree of crystallinity in Table V may be compared with those in Tables III and IV for samples that were crystallized rapidly in dynamic mode at elevated temperatures. The degree of crystallinity of all systems is very close, although crystallinity is slightly greater in the rapidly crystallized samples than in the slowly crystallized samples. How-

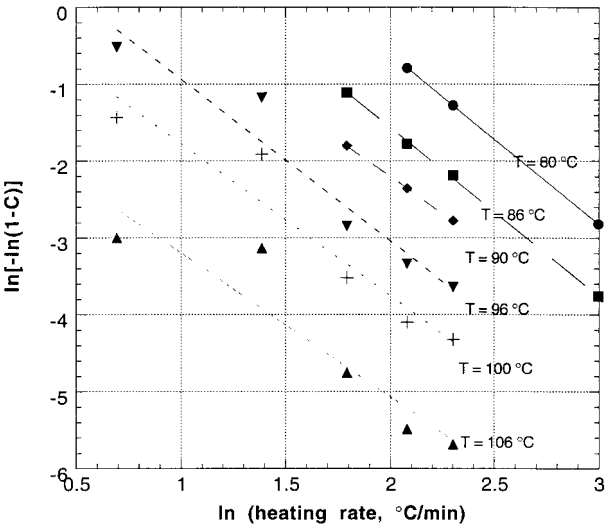

Figure 12 Plot of $\ln[-\ln(1 - C)]$ as a function of $\ln \phi$ for various values of temperature in unreinforced PHB.

ever, while this slight disparity is observed in all systems, the shift in crystallinity values is within the uncertainty in the measurements. It is an noteworthy conclusion of this work that there is no significant correlation between crystallization rate and ultimate degree of crystallinity for PHB and PHB/9%HV composites. This observation suggests that the thermal method used in the dynamic melt crystallization experiments provides ample time for slow secondary crystallization processes that perfect crystals rapidly formed at high temperatures. Secondary crystallization or annealing is always possible for PHB and PHB/HVs that are stored at room temperature, as this temperature is above the glass transition temperature for these materials.

Modeling of Crystallization Kinetics

The kinetics of crystallization were analyzed using a nonisothermal Avrami method. This analysis is based on the Ozawa equation for dynamic crystallization[19]:

$$\ln\{-\ln[1 - C(T)]\} = \chi - n \ln \phi, \qquad (1)$$

where $C(T)$ is the crystalline volume fraction as a function of temperature during the DSC scan, χ is a parameter that depends on nucleation and growth rates, n is the well-known Avrami exponent, and ϕ is the heating rate. The value of the Avrami exponent provides direct information about the nucleation mechanism and growth geometry of the polymer crystals.

A plot of $\ln\{-\ln[1 - C(T)]\}$ as a function of $\ln \phi$, or nonisothermal Avrami plot, is used to determine the Avrami exponent, n. The quantity $\ln\{-\ln[1 - C(T)]\}$ is plotted as a function of $\ln \phi$ for selected values of temperature, and the absolute value of the slope is the value of the Avrami exponent. Figure 12 shows an Avrami plot for unreinforced PHB. The slopes of the best-fit lines for the various temperatures are approximately equal, indicating that nucleation mechanism and growth geometry do not change significantly during the dynamic crystallization process. The average value of the slope for temperatures between 80 and 106°C is 2.0 ± 0.1. Possible interpretations for this exponent are two-dimensional circular growth, which is instantaneously nucleated or one-dimensional linear growth, which is sporadically nucleated. We recall that optical microscopy of unreinforced PHB showed significant sporadic nucleation as well as spherulitic growth. This observation is at odds with both possible interpretations of the Avrami exponent.

Figure 13 shows the nonisothermal Avrami plot for PHB reinforced with 20 wt % Kraft fibers. Again, the slopes of all curves are approximately equal and the average value is 2.8 ± 0.1. A possible interpretation of a noninteger n value is crystallization, in which a combination of mechanisms is acting.[15,20,21] An Avrami exponent of 3.0 may be attributed to either two-dimensional sporadic

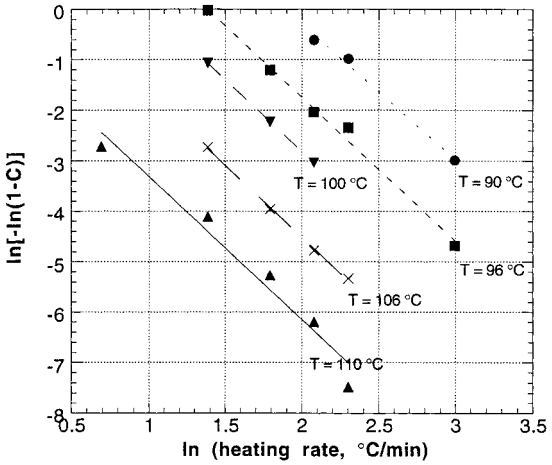

Figure 13 Plot of $\ln[-\ln(1 - C)]$ as a function of $\ln \phi$ for various values of temperature in PHB reinforced with 20% bleached kraft fiber.

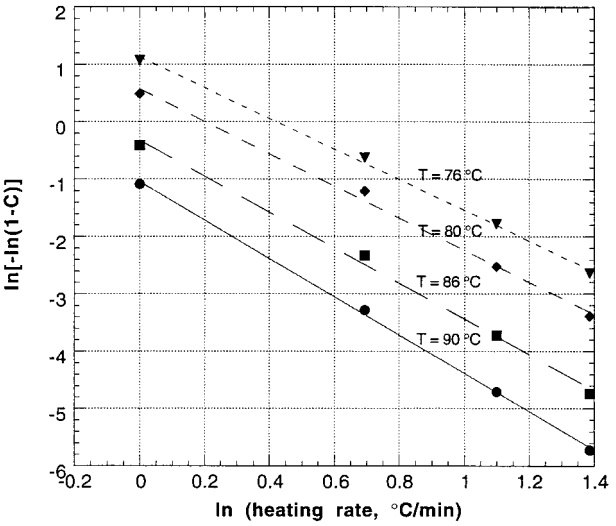

Figure 14 Plot of $\ln[-\ln(1 - C)]$ as a function of $\ln \phi$ for various values of temperature in unreinforced PHB/9%HV.

growth or to three-dimensional instantaneously nucleated growth. If slow secondary crystallization (annealing) occurred in addition to the primary process, the value of the Avrami exponent would be slightly depressed. Thus, the noninteger n value may reflect a combination of nucleation mechanisms or a significant contribution of annealing to the crystallization process. Figure 14 shows the nonisothermal Avrami plot for unreinforced PHB/9%HV copolymer. The slope of the constant temperature lines is 3.0 ± 0.3. As stated above, this exponent is consistent with either two-dimensional sporadically nucleated growth or three-dimensional instantaneously nucleated growth.

It is interesting that the Avrami exponent of crystallization is greater for reinforced PHB than for PHB. According to the derivation of the Avrami model, larger values of n are associated with either less constrained growth or with thermal nucleation (the nucleation of crystals throughout the crystallization process). Yet optical microscopy observations indicate that growth is more, not less, constrained in fiber-reinforced PHB as compared with unreinforced PHB. Furthermore, in the reinforced case more nuclei are observed to form instantaneously rather than sporadically with time. This same anomalous shift in Avrami exponent has been observed in other reinforced polymers displaying an increased crystallization rate.[15]

It is also interesting that the nucleation mechanism and/or growth geometry are affected by the introduction of HV units in PHB crystals, as reflected by the change in Avrami exponent from 2.0 for PHB to 3.0 for PHB/9%HV. Although PHB/9%HV is thought to crystallize in the PHB unit cell (see above), the kinetics of crystallization are significantly affected by the introduction of HV units. The observed increase in n may reflect a more thermal, or sporadic, nucleation or a less constrained growth geometry. If the density of nuclei were reduced in the copolymer as compared with PHB, less constrained crystal growth would result. A depression in nucleation density is reasonable in PHB/9%HV, because of the difficulty in creating nuclei of a critical size resulting from the presence of HV units along the PHB chain.

SUMMARY

This study has examined the effects of fiber reinforcement on the crystallization of PHB, PHB/9%HV, and PHB/24%HV. Optical microscopy showed that polymer crystals were heterogeneously nucleated on the fiber surface, thus increasing nucleation density. This observation is true for crystallization from the glassy state (recrystallization or cold crystallization) and for crystallization from the melt.

Modulated differential scanning calorimetry was used to determine the dynamic crystallization temperature of fiber-reinforced PHB and PHB/HVs from the melt and from the glass. Bleached Kraft, TMP, and microcrystalline cellulose reinforcements significantly increase the crystallization rate, as reflected by changes in the melt and cold crystallization temperatures. The strong effect of reinforcing fibers on crystallization rate is presumed to be due to increased heterogeneous nucleation on the fiber surface. Nucleation rates in unreinforced PHAs are very slow because of the purity of these compounds and are even slower in the copolymers, by the inclusion of comonomers during cocrystallization. Although reinforcing fibers significantly increased the crystallization temperature of PHAs, the final degree of crystallinity, or crystalline fraction, was the same in rapid and in slow crystallizing systems. Rapid crystallization does not produce a less perfect crystalline phase.

Examination of the nonisothermal Avrami crystallization kinetics reveals a shift in the value of the Avrami exponent as a result of fiber reinforcement and cocrystallization. The shift in the value of the exponent reflects a change in nucle-

ation mechanism and growth geometry due to the presence of fiber reinforcement.

The authors gratefully acknowledge the work of Dr. David Johnson of National Renewable Energy Laboratory in performing the gel permeation chromatography work and recognize the insights and support of Dr. Paul Weaver of the National Renewable Energy Laboratory. We also thank Professor John Simonsen of Oregon State University for sharing his plastics compounding equipment with us. Modulated Differential Scanning calorimetry was developed by, and is a trademark of, TA Instruments, Inc. Use of this technique by the authors does not constitute an endorsement of the product.

REFERENCES

1. K. A. Pirrotta, M.S. Thesis, Princeton University, June 1993.
2. M. Scandola, G. Ceccorulli, M. Pizzoli, and M. Gazzano, *Macromolecules,* **25,** 1405 (1992).
3. W. J. Orts, R. H. Marchessault, and T. L. Bluhm, *Macromolecules,* **24,** 6435 (1991).
4. M. Kunioka, A. Tamaki, and Y. Doi, *Macromolecules,* **22,** 694 (1989).
5. S. J. Organ and P. J. Barham, *Polymer,* **34,** 459 (1993).
6. P. Gatenholm, J. Kubat, and A. Mathiasson, *J. Appl. Polym. Sci.,* **45,** 1667 (1992).
7. H. Bauer and A. J. Owen, *Colloid Polym. Sci.,* **266,** 241 (1988).
8. E. A. Dawes, *Biosci. Rep.,* **8,** 537 (1988).
9. R. A. Gross, C. DeMello, R. W. Lenz, H. Brandl, and R. C. Fuller, *Macromolecules,* **22,** 1106 (1989).
10. S. Akhtar, C. W. Pouton, and L. Notarianni, *Polymer,* **33,** 117 (1992).
11. P. J. Barham, *J. Mater. Sci.,* **19,** 3826 (1984).
12. T. L. Bluhm, G. K. Hamer, R. H. Marchessault, C. A. Fyfe, and R. Veregin, *Macromolecules,* **19,** 2871 (1986).
13. N. Kamiya, M. Sakurai, Y. Inoue, R. Chujo, and Y. Doi, *Macromolecules,* **24,** 2178 (1991).
14. G. P. Desio and L. Rebenfeld, *J. Appl. Polym. Sci.,* **44,** 1989 (1992).
15. V. E. Reinsch and L. Rebenfeld, *J. Appl. Polym. Sci.,* **52,** 649 (1994).
16. S. Bloembergen, D. A. Holden, G. K. Hamer, T. L. Bluhm, and R. A. Marchessault, *Macromolecules,* **19,** 2865 (1986).
17. N. Kamiya, Y. Inoue, Y. Yamamoto, R. Chujo, and Y. Doi, *Macromolecules,* **23,** 1313 (1990).
18. TA Instruments, Inc., *Modulated DSC Application Brief,* Brief number MDSC-7.
19. T. Ozawa, *Polymer,* **19,** 1142 (1978).
20. G. P. Desio and L. Rebenfeld, *J. Appl. Polym. Sci.,* **45,** 2005 (1992).
21. S. A. Jabarin, *Polym. Eng. Sci.,* **29,** 1259 (1989).